This article has been accepted for publication in a future issue of this journal, but has not been fully edited.
Content may change prior to final publication in an issue of the journal. To cite the paper please use the doi provided on the Digital Library page.

Heart rate variability estimation in Photoplethysmography signals using Bayesian learning approach

Ahmed Alqaraawi, Ahmad Alwosheel and Amr Alasaad

King Abdulaziz City for Science and Technology
Center of Excellence in Telecommunication Applications
Riyadh-Saudi Arabia
E-mails: aqaraawi@kacst.edu.sa, aalwosheel@kacst.edu.sa, alasaad@kacst.edu.sa

Published in Healthcare Technology Letters; Received on xxx; Revised on xxx.

Heart Rate Variability (HRV) has become a marker for various health and disease conditions. Photoplethysmography (PPG) sensors integrated in wearable devices such as smart watches and phones are widely used to measure heart activities. HRV requires accurate estimation of time interval between consecutive peaks in the PPG signal. However, PPG signal is very sensitive to motion artifact which may lead to poor HRV estimation if false peaks are detected. In this paper, we propose a probabilistic approach based on Bayesian learning to better estimate HRV from PPG signal recorded by wearable devices and enhance the performance of the AMPD algorithm used for peak detection. Our experiments show that our approach enhances the performance of the AMPD algorithm in terms of number of HRV related metrics such as sensitivity, positive predictive value, and average temporal resolution.

1. Introduction: The Heart Rate Variability (HRV) is a measure of variation in time duration between consecutive heart beats. HRV has used widely as an indicator for stress, health and various disease conditions [1], [2]. This paper presents a probabilistic approach for estimating HRV from Photoplethysmography (PPG) signal recorded by wearable devices.

Photoplethysmography (PPG) sensors integrated in wearable devices such as smart watches and phones are widely used nowadays to provide a convenient way to measure heart activities. Average heart rate can be measured by many commercial wearable gadgets. However, motion artifact still presents a challenging problem in estimating the heart rate variability in PPG signals collected by wearable devices [3], [4], [5], [6], [7]. This problem motivates researchers to propose algorithms that enhance the accuracy of HRV measured by those wearable PPG sensors, and enable reliable assessment of the health conditions and provide correct diagnoses.

In a PPG signal, the location of a peak represents the instant of time at which a heartbeat occurs. Thus, the computation of HRV requires accurate identification of the location of peaks in the PPG signal, which consequently leads to precise computation of time intervals between consecutive heartbeats. Many relevant features can be derived from the HRV measurement such as pNN50 and RMSSD. Researchers have shown that these features can imply valuable information about various health conditions [8]. These features, however, are sensitive to any small error in identifying the correct location of peaks. Hence, accurate peak detection in the PPG signal collected by a portable devise is crucial.

The nature of a PPG signal makes HRV measurements a challenging problem, especially when using a portable PPG sensor. As shown in Fig. 1, the first wave in the PPG waveform is called systolic peak and the second one is called diastolic peak. Aortic notch or Dicrotic notch is a small downward deflection in the arterial pulse that separates systolic and diastolic phase. The first peak (systolic) represents the instant of time corresponding to a heart beat, also known as R-peak. A small motion artifact can result in the diastolic peak having a higher amplitude than the systolic peak (e.g., Fig. 8), which may lead to erroneous HRV estimation if the diastolic peak is detected as the instant of heart beat.

In this paper, we present an adaptive real-time probabilistic approach that employs Bayesian learning to estimate HRV from PPG signal recorded by wearable devices. In particular, our approach uses an algorithm called Automatic Multi scale-based Peak Detection (AMPD) [9] along with a probabilistic method to enhance its performance and provide a better HRV estimation. The proposed approach provides a soft decision on every sample in the PPG signal. We adopt a probabilistic approach that allows us to compute the probability of having a peak at every sample, and make a decision whether a peak exists in that sample by comparing the computed probability with a configured threshold. Our experiments show that the proposed algorithm enhances the AMPD algorithm with respect to a number of HRV related performance metrics such as sensitivity, positive predictive value, and average temporal resolution.

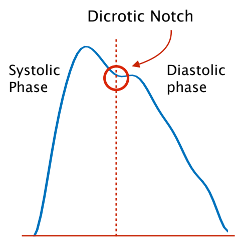

Figure 1. Typical PPG waveform

2. AMPD algorithm background: This section explains briefly the algorithm proposed by Scholkmann *et al.* [9]. The algorithm is called Automatic Multi scale-based Peak Detection (AMPD), and aims to detect signal peaks by analyzing the local maxima scalogram (LMS) of periodic or quasi-periodic signals. Let $X = [x_1, x_2, ..., x_N]$ be a uniformly sampled signal containing components of a PPG signal. AMPD algorithm calculates the LMS using a moving window approach, whereby the window length w_k is varied ($w_k = 2k|_{k=1,2,..,L}$), where k is defined as a scale in which the PPG signal is analyzed (analysis resolution). A scale could be mapped to a frequency for convenience. L represents the number of scales in the scalogram and should be defined to cover the range of frequencies that are useful for PPG signal analysis (typically, $L = 2f_s$, is sufficient to include HR as low as *30 bpm*, where f_s is the sampling frequency). In other words, the moving window w_k is varied at every scale k to cover different resolutions of the PPG signal. Then, a comparison criterion is performed at

This article has been accepted for publication in a future issue of this journal, but has not been fully edited.
Content may change prior to final publication in an issue of the journal. To cite the paper please use the doi provided on the Digital Library page.

every scale k on the PPG signal for $i = k+2, ..., N-k+1$ to search for local maxima as follows.

$$m_{k,i} = \begin{cases} 1 & x_{i-1} > x_{i-k-1} \;\&\; x_{i-1} > x_{i+k-1} \\ 0 & \text{otherwise} \end{cases} \tag{1}$$

This operation results in a matrix M, where

$$M = \begin{pmatrix} m_{1,1} & m_{1,2} & \cdots & m_{1,N} \\ m_{2,1} & m_{2,2} & \cdots & m_{2,N} \\ \vdots & \vdots & \ddots & \vdots \\ m_{L,1} & m_{L,2} & \cdots & m_{L,N} \end{pmatrix} = (m_{k,i}) \tag{2}$$

where the k^{th} row contains the value for the window length w_k. The ones in matrix M represent locations of local maxima (or the indices where potential PPG R-peaks exist) at every scale k. A PPG sample is decided to be a peak when there exists 1's for every scale k at a specific instance of time (a column in the matrix M).

3. Algorithm Description: The proposed algorithm consists of two parts. Part 3.1 uses a slight modification to the output of the AMPD algorithm explained in Section 2 and exploits a model that has been built using a historical previous knowledge about R-peaks, while Part 3.2 further enhances the performance of AMPD using a probabilistic approach based on Bayesian learning. Details of the two parts are presented in the next subsections and demonstrated in Fig. 2 and Fig. 3.

Definition of used notations:
Let us start by denoting t_j as the instant of time at which the j^{th} R-peak occurred. We can also define the process r as the inter-arrival time between two consecutive peaks (also known as RR-intervals), namely:

$$r_j = t_{j+1} - t_j \tag{3}$$

Another way to represent PPG peaks is by considering a process d given by the difference between consecutive RR-intervals, i.e.,

$$d_j = r_{j+1} - r_j \tag{4}$$

The latter definition is helpful for estimating the occurrence of a next peak as will be seen next.

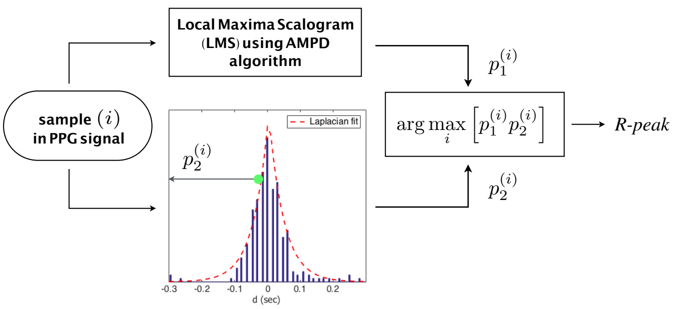

Figure 2. Description of the algorithm design of Part 3.1

3.1. AMPD output modification and prior probabilistic knowledge: The AMPD algorithm works well even when a white noise is presented in a signal. Applying the algorithm to a PPG signal, which has a quasi-periodic nature, provides promising results. However, the AMPD performance degrades when the signal is corrupted with motion artifact. This is because the probabilistic characteristics of such artifact differs from the white noise.
In the AMPD algorithm, a sample is decided to be a peak if there exist ones for every scale k (i.e. all the elements in column i = 1). We modify this condition by computing p_1 of sample i as a ratio of the number of ones in column i in the matrix M to the total number of rows L, that is

$$p_1^{(i)} = \frac{\sum_{k=1}^{L} m_{k,i}}{L} \tag{5}$$

An enhancement could be achieved by calculating the probability of having a peak at sample i by incorporating historical previous knowledge about R-peaks. In [10], authors show that the Laplacian model exhibits the best fit for analyzing the d process. Based on their results, the probability p_2 of sample i to be a peak using Laplacian distribution is given by

$$p_2^{(i)} = \frac{1}{2b} \exp\left(-\frac{|d_i - \mu|}{b}\right) \tag{6}$$

Since the decision is not yet made whether sample i is a peak, d_i definition in Eq. 6 slightly differs from the general one in Eq. 4. It is defined here as $d_i = r_i - r_{last}$, where r_i represents the difference between sample i and the last detected peak, while r_{last} represents the last recorded RR-interval from the last cycle. μ in Eq. 6 is defined as the median. From the observed historical data of PPG signals, it is reasonable to assume that μ equals to zero. b in Eq. 6 is a scalar parameter calculated as

$$b = \frac{1}{K} \sum_{j=1}^{K} |d_j - \mu|, \tag{7}$$

where K is the number of records of the process d. To that end, one can build the decision criterion by considering the two parameters p_1 and p_2, based on the maximum probability of all samples that fall within the range of interest. i.e.,

$$Peak = \arg\max_i \left[p_1^{(i)} p_2^{(i)}\right] \tag{8}$$

However, we can enhance the accuracy of a peak detection by accounting for the variation of the heart rate. To consider such cases, the constructed model should be dynamic and updated on the fly. For that reason, a Bayesian inference is proposed in the next subsection.

3.2. Probabilistic analysis and Bayesian inference formulation of the problem: Let us start by assuming that the probability of having a peak at sample i is θ_i. θ_i can be initially calculated using Eq. 6 ($i.e., \theta_i = p_2^{(i)}$). However, having a decision merely using θ_i may not be the best thing to do, given that we can learn from the incoming data. Thus, we can formulate the problem using Bayesian inference as follows:

$$posterior_{(i)} = P(\theta_i \mid AMPD_{output(i)}) = \\ P(AMPD_{output(i)} \mid \theta_i) \cdot P(\theta_i)_{prior} \tag{9}$$

Considering the term $P(\theta_i)_{prior}$ in Eq. 9, it is the prior probability distribution of θ_i. We aim at finding a distribution to model $P(\theta_i)_{prior}$ that initially considers the probability computed in Eq. 6 as the expected value for this distribution and can be easily updated during the learning process. We used the Beta function to achieve this goal. To see why the Beta function is good to model $P(\theta_i)$, one can observe that such model results in a positively skewed probability distribution (skewed to the left) when θ_i is low (which is the case for a sample i that is close to last detected peak), while it is negatively skewed probability distribution (skewed to the right) when θ_i is high (which is the case when sample i is close to next expected peak). Samples that are in the middle of consecutive expected peaks result in a probability distribution for θ_i that is close to the uniform distribution. Such Beta function behavior is illustrated in Fig. 4. We observe that such statistical behavior of the

This article has been accepted for publication in a future issue of this journal, but has not been fully edited.
Content may change prior to final publication in an issue of the journal. To cite the paper please use the doi provided on the Digital Library page.

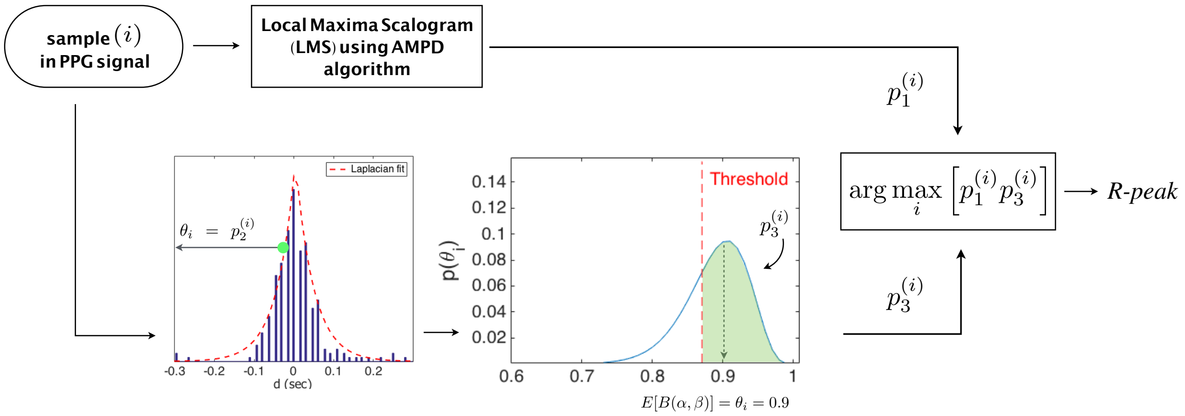

Figure 3. Description of the algorithm design of Part 3.2

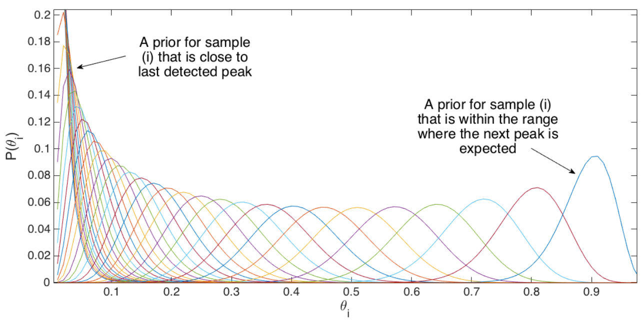

Figure 4 *Modeling for the prior probability distribution ($P(\theta_i)_{prior}$) as Beta function*

Beta distribution can be used to model $P(\theta_i)_{prior}$ very well. Hence, we can consider

$$P(\theta_i)_{prior} = \frac{\Gamma(\alpha+\beta)}{\Gamma(\alpha)\Gamma(\beta)} \theta_i^{\alpha-1}(1-\theta_i)^{\beta-1} \tag{10}$$

where Γ is the Gamma function, and can be obtained in a tabular form corresponding to the Gamma probability distribution. Note that $\frac{\Gamma(\alpha+\beta)}{\Gamma(\alpha)\Gamma(\beta)}$ is a normalized constant to ensure that the total probability integrates to 1. α and β are called hyper-parameters that control the shape of the distribution. We need to set those parameters such that they properly characterize a prior probability distribution for every sample i. We know that

$$E[\theta_{i-prior}] = \alpha/_{\alpha+\beta}, \tag{11}$$

when $\theta_{i-prior}$ follows Beta probability distribution. We initially sets this expectation value to be $E[\theta_{i-prior}] = p_2^{(i)}$. Further, we assume that $(\alpha+\beta)$ is constant, where the constant can be configured according to the implementation design. By plugging the values of $p_2^{(i)}$ and the constant $(\alpha+\beta)$ into Eq. 11, we get the desired parameters α and β that characterize the Beta distribution for a specific sample i. To summarize the discussion above, the $P(\theta_i)_{prior} \sim B(\alpha,\beta)$ with expectation value of $\theta_{i-prior}$ equals to $p_2^{(i)}$.

Going back to Eq. 9, let us consider the likelihood $P(AMPD_{output(i)} \mid \theta_i)$, where $AMPD_{output(i)}$ is considered here as a binary variable representing outputs from the AMPD algorithm. In other words, $AMPD_{output(i)}$ is 1 when $p_1^{(i)}$ in Eq. 5 equals to 1 and zero otherwise. Since we assume independent θ_i for every sample i (i.e., θ_i's are iid), we can think of the binary output of the AMPD algorithm at each sample i as an outcome of a Bernoulli experiment, wherein each sample i has its own θ_i. Thus, we can write

$$P(AMPD_{output(i)} \mid \theta_i) = \theta_i^n (1-\theta_i)^{1-n} \quad , \text{for } n \in \{0,1\} \tag{12}$$

Substituting Eq. 10 and Eq. 12 into Eq. 9, we get the the posterior probability distribution of θ_i as a new Beta distribution $B(\alpha', \beta')$, i.e.;

$$posterior_{(i)} = B(\alpha', \beta') = \theta_i^{n+\alpha-1}(1-\theta_i)^{\beta-n} \tag{13}$$

In other words, if the binary output of the AMPD algorithm at sample i equals to $n=1$, then $\alpha' = \alpha+1$ and $\beta' = \beta$, while if $n=0$, then $\alpha' = \alpha$ and $\beta' = \beta+1$. It turns out that this is a simple and compact way to update the parameters of $posterior_{(i)}$ at every cycle.

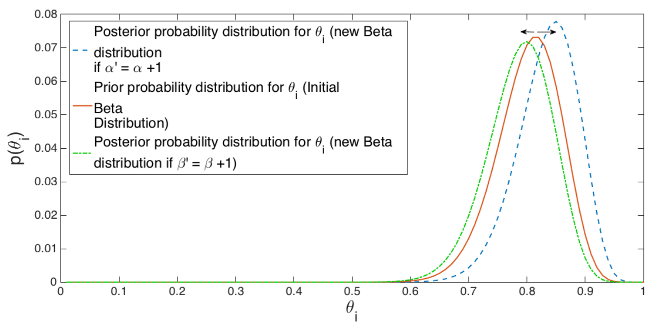

Figure 5. Explanation of the learning procedure

3.3. Learning procedure: We define a cycle as the time interval between two peaks. During that cycle, the task is to search for the next peak. In the very first cycle of the PPG sampled data, prior probability distribution for θ_i are initiated for every sample falls within the range of interest exploiting information acquired from Eq. 6. In the next cycle, the posterior probability distribution for θ_i ($posterior_{(i)}$) is computed by updating the Beta function with $+1$ for α or β depending on the $AMPD_{output(i)}$ for that specific sample. Practically, having $\alpha' = \alpha+1$ results in shifting the Beta function curve to the right (increases the confidence for that sample being a peak), while having $\beta' = \beta+1$ results in shifting Beta function curve to the left (decreases the confidence for that sample being a peak). Since this procedure is repeated for every cycle, those samples corresponding to the most probable peak locations will have higher expected value as the distribution of their posteriors will be skewed to the right. Demonstration of this learning procedure is depicted in Fig. 5.

3.4. R-peak decision criterion: The decision of a new peak is made by considering two terms. Firstly, the ratio $p_1^{(i)}$ acquired from $AMPD$ algorithm in Eq. 5. Secondly, the confidence value $p_3^{(i)}$ of the corresponding $posterior$ of sample i, where $p_3^{(i)}$ is calculated as

$$p_3^{(i)} = \int_{threshold}^{1} posterior_{(i)} d\theta_i = \int_{threshold}^{1} Beta(\alpha', \beta') d\theta_i, \tag{14}$$

where $threshold$ can be configured empirically. $p_3^{(i)}$ value represents the confidence that sample i is R-peak. Note that $posterior_{(i)}$ follows Beta function with a pdf that sums to one. The proposed algorithm makes a decision on R-peak by applying Eq. 15 below for all considered samples within the range of interest as follows

$$Peak = \arg\max_i \left[p_1^{(i)} p_3^{(i)} \right] \tag{15}$$

Fig.6 illustrates the approach of calculating the value p_3 of sample i.

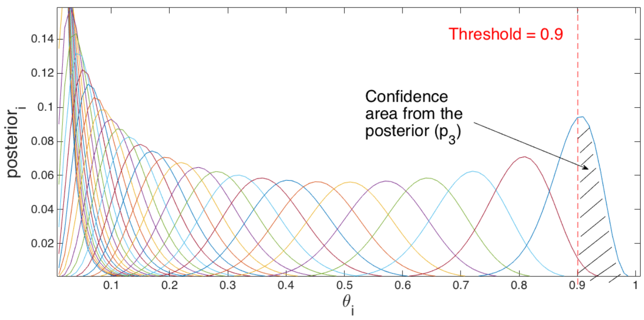

Figure 6 *The posterior probability distribution of θ_i for sample i. Every graph in the figure represents $posterior_{(i)}$ for sample i.*

We note that by incorporating information from AMPD algorithm in Part 3.1, we are adding an independent source of information as input to the decision criterion. Moreover, the output from AMPD helps the proposed algorithm to avoid error propagation, which may happen since decision on the next peak relies on the previously detected peak.

4. Evaluation: For the purpose of evaluating the proposed approach, the ECG signal was recorded using Zephyr BioHarness3 chest strap with sampling rate 250Hz, from which we computed the instants of time at which we have heartbeats. The ECG results are used as a ground-truth to PPG signal algorithms under comparisons. The PPG signals were collected from Empatica PPG sensor with a sampling rate 64Hz.

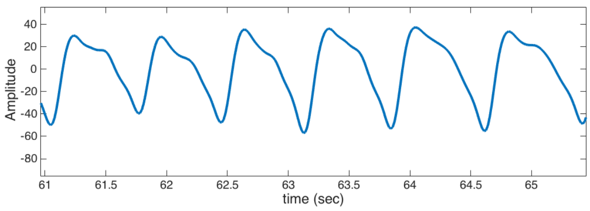

Figure 7. A sample of PPG signal: artifact-free

4.1. Experimental setup and performance metrics: The recorded PPG data were processed and analyzed using MATLAB simulation environment, wherein the authors of this paper were the subjects of the experiments. We evaluated the performance in two cases. In the first case, We considered 5 minutes recording of artifact

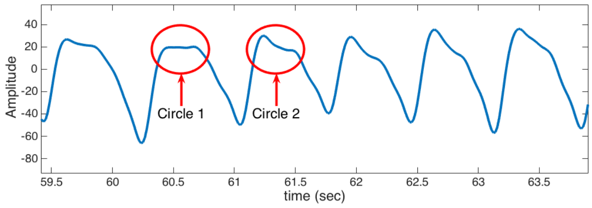

Figure 8. A sample of PPG signal: corrupted with some artifacts

free PPG signal. Fig. 7 shows a sample of the PPG signal used in this experiment. In order to simulate the artifact in PPG signals, we considered a spike signal that follows Poisson arrivals with mean 0.25 (arrival/second) and signal amplitudes that vary with different signal to noise ratio (SNR). In the second case, we considered 8 minutes PPG signal recording, wherein the subjects were performing different activities including: resting, walking and slow hand movement in vertical, horizontal and circular direction. This kind of physical motion results in some artifact in the PPG signal and a baseline wander.

We compared our proposed algorithm against AMPD algorithm in terms of three performance metrics: Sensitivity (Se), positive predictivety ($+P$), and Average Temporal Resolution (ATR). Se and $+P$ metrics were proposed by Advancement of Medical Instrumentation (AAMI) [11]. The two metrics assess the performance in terms of two expected errors: missing peaks or detecting non existed peaks (phantoms), respectively. The two metrics are defined as:

$$Se = \frac{TP}{TP + FN} \tag{16}$$

and

$$+P = \frac{TP}{TP + FP} \tag{17}$$

These metrics are evaluated within an acceptance range, where the acceptance range is defined as half the time lapses between a peak and its predecessor and successor peaks in the PPG signal. When peaks are detected within the acceptance interval, they are considered as True Positives (TP). Detection of false peaks (phantoms) are referred to False Positives (FP). Missed peaks within the acceptance interval are marked as False Negatives (FN). In this sense, sensitivity (Se) indicates the percentage of true peaks that were correctly detected by the algorithm over all peaks, while positive predictive value ($+P$) indicates the percentage of true peaks that were correctly detected but are not phantoms. By temporal resolution, we refer to the time accuracy which the detection of a peak using the proposed approach is compared to the ground truth peak, which is acquired from ECG signal. In other word, the difference between the instant in which a peak is detected using the proposed approach ($T1$) and the ground truth value ($T2$) is computed. Taking into consideration that the PPG signal contains numerous peaks, the Average Temporal Resolution (ATR) is computed as shown in Eq. 18.

$$ATR = \frac{\sum_{j=1}^{N} |T1_{(j)} - T2_{(j)}|}{N}, \tag{18}$$

where N is the total number of peaks in the signals.

Table 1 ATR: performance evaluation for case 2

Approach	ATR
Our proposed approach	$6.8ms$
AMPD	$45.2ms$

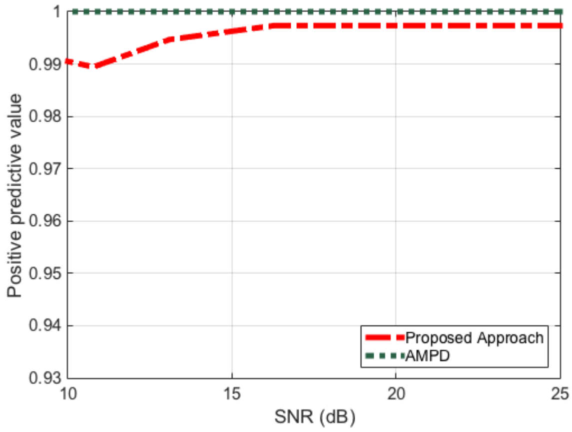

Figure 9. Performance evaluation: Positive predictive value

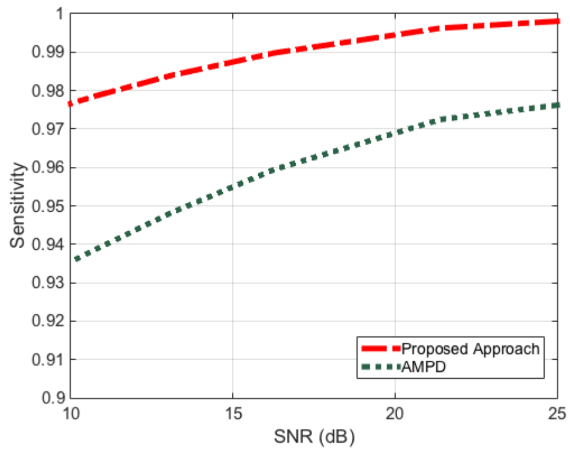

Figure 10. Performance evaluation: Sensitivity

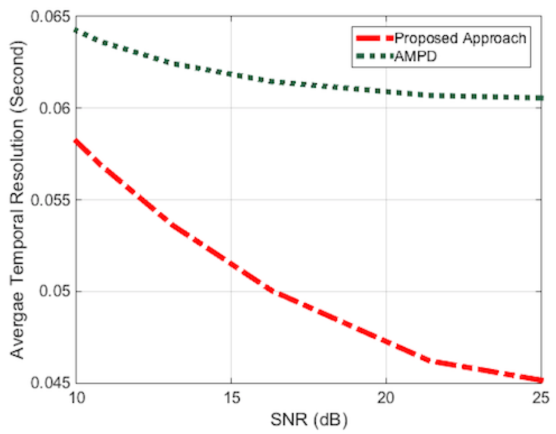

Figure 11. Performance evaluation: Average temporal resolution (ATR)

4.2. Results and Discussion: The results of the first case are shown in Fig. 9, Fig. 10 and Fig. 11, while the results of the second case are shown in Table 1.

PPG signal is usually exposed to different types of noise and artifacts. Fig. 8 shows a typical PPG signal where noise exists at part of the signal. Circle 2 represents a part of the signal where only one peak exists within a cycle. Such peak can be easily detected by several algorithms. On the other hand, Circle 1 shows a situation where the peak is hard to be detected. Our approach overcomes this problem by a applying Bayesian-based algorithm that utilizes prior knowledge about the instant of the occurrence for several previous peaks.

In the first case, the results show a comparable performance between AMPD and our proposed algorithm in term of positive predictive value $+P$ (Fig. 9). However, our proposed algorithm outperforms AMPD in terms of Se and ATR as shown in Fig. 10 and Fig. 11, respectively. We can observe from Fig. 10 that as SNR value decreases, the difference in Se (which is related to the number of missed peaks) increases between the two approaches. Having a high conservative algorithm when making a decision on a peak, such as AMPD, results in selecting only peaks with high confidence. Meaning that AMPD decides a sample i is a peak when this detected peak represents a global maximum for all scales. For this reason, the AMPD algorithm misses some "true peaks". Therefore, AMPD has high $+P$ but relatively lower Se. Depending on the application at hand, $+P$ metric may be very important, and in that case, a conservative approach for detecting peaks such as AMPD may be desirable. In any case, our approach provides a very comparable result for the case of +P, but significantly enhances the performance of Se, yielding to superior overall performance. In Fig. 11, the ATR values of AMPD increase as SNR level decreases. The proposed approach shows better performance for different SNR levels. It is observed that the difference between ATR values is decreasing as more noise is introduced to the signal.

The results of the second case are shown in Table 1. The ATR difference between the two approaches is around 38 msec, while the Se and $+P$ values are similar. Achieving better accuracy in temporal resolution is important as this error represents the standard deviation in heart rate that directly reflects the HRV. In [12], authors present a quantitative systematic review of normal values for short-term heart rate variability in healthy adults. Authors showed in a tabular form a summary data including the overall range in values for each of the HRV measures. One of the important HRV measures is the SDNN (the standard deviation of the RR intervals). It is known that SDNN is directly affected by the number of missed peaks (which represents the Se), phantoms (which represents $+P$) and the temporal accuracy of the detected peak (which is represented by ATR). It has been shown in [12] that SDNN ranges between (32-93)ms with mean 50ms according to 27 studies surveyed. Table 2 shows the impact of ATR on some HRV measures including SDNN values. We can observe that, for example, SDNN computed by AMPD is outside the range of SDNN of healthy adults according to the survey in [12]. Thus, errors in peak detections may provide SDNN value that yields to erroneous diagnoses and physiological interpretation.

Table 2 HRV measurements for case 2

HRV Metric	ECG	Our approach	AMPD
SDNN	86.3	87.5	204.8
SDANN	45.9	53.6	172.2
pNN50	18.7	24.2	63.3
RMSSD	54.6	62.7	265.9
SDNNi	67.4	65	103.5
Average HR	68.9	69	68.1

5. Conclusion: Our proposed approach uses a Bayesian learning algorithm to estimate HRV from PPG signals. This approach enhances the performance of AMPD algorithm and enables better HRV estimation when PPG is distorted with artifact. Our experiments show that the proposed approach has a comparable performance with the AMPD in terms of sensitivity and positive predictive value. However, it outperforms the AMPD in terms of average temporal resolution. In future work, we shall develop an accurate model for the prior probability distribution using historical observations of RR-intervals from a large dataset with different scenarios. We shall also attempt to mathematically characterize the noise that is typically associated with the PPG signals collected by wearable sensors.

6. Funding and Declaration of Interests: This work was supported by the Center of Excellence in Telecommunication Applications at King Abdulaziz City for Science and Technology, National Science, Technology and Innovation plan (NSTIP) grant numbers 34-987 and 34-988.
Conflict of interest: None declared

7 References

[1] Choi, J. and Gutierrez-Osuna, R. : "Removal of respiratory influences from heart rate variability in stress monitoring," *IEEE Sensors Journal*, vol. 11, no. 11, pp. 2649-2656, Nov 2011.

[2] Tamura, T , Maeda, Y., Sekine, M., and Yoshida, M. : "Wearable photoplethysmographic sensors - past and present," *Electronics*, vol. 3, no. 2, pp. 282-302, 2014.

[3] Yousefi, R., Nourani, M., Ostadabbas, S., and Panahi, I. : "A motion-tolerant adaptive algorithm for wearable photoplethysmographic biosensors," *IEEE Journal of Biomedical and Health Informatics*, vol. 18, no. 2, pp. 670-681, March 2014.

[4] Ram, M., Madhav, K., Krishna, E., Komalla, N., and Reddy, K. : "A novel approach for motion artifact reduction in ppg signals based on as-lms adaptive filter," *IEEE Transactions on Instrumentation and Measurement*, vol. 61, no. 5, pp. 1445-1457, May 2012.

[5] Zhang Z., "Photoplethysmography-based heart rate monitoring in physical activities via joint sparse spectrum reconstruction," *IEEE Transactions on Biomedical Engineering*, vol. 62, no. 8, pp. 1902-1910, Aug 2015.

[6] Zhang, Z., Pi, Z., and Liu, B. : "Troika: A general framework for heart rate monitoring using wrist-type photoplethysmographic signals during intensive physical exercise," *IEEE Transactions on Biomedical Engineering*, vol. 62, no. 2, pp. 522-531, Feb 2015.

[7] Krishnan, R., Natarajan, B., and Warren, S. : "Two-stage approach for detection and reduction of motion artifacts in photoplethysmographic data," *IEEE Transactions on Biomedical Engineering*, vol. 57, no. 8, pp. 1867-1876, Aug 2010.

[8] Task Force of the European Society of Cardiologyetal, "Heart rate variability standards of measurement, physiological interpretation, and clinical use," *Eur Heart J*, vol. 17, pp. 354-381, 1996.

[9] Scholkmann, F., Boss, J., and Wolf, M. : "An efficient algorithm for automatic peak detection in noisy periodic and quasi-periodic signals," *Algorithms*, vol. 5, no. 4, pp. 588-603, 2012.

[10] Quer, G., and Rao, R. : "A bayesian model of heart rate to reveal real- time physiological information," in *14th International Conference on e-Health Networking, Applications and Services*. pp. 223–229, 2012,

[11] A.-A. EC57, "Testing and reporting performance results of cardiac rhythm and ST segment measurement algorithms," *Association for the Advancement of Medical Instrumentation*, Arlington, VA, 1998.

[12] Nunan, D., Sandercock, GR, Brodie, DS, :?A quantitative systematic review of normal values for short-term heart rate variability in healthy adults,? *Pacing Clin. Electrophysiol.*, vol. 33, no. 11, pp. 1407-17, Nov 2010.